Japanese Journal of Applied Physics

The Japan Society of Applied Physics

REGULAR PAPER

A simple analysis of polarization reversal of ferroelectric capacitor demonstrating negative capacitance-like behavior

To cite this article: Eisuke Tokumitsu 2020 *Jpn. J. Appl. Phys.* **59** SCCB06

Japanese Journal of Applied Physics **59**, SCCB06 (2020) **REGULAR PAPER**
https://doi.org/10.7567/1347-4065/ab4cfc

A simple analysis of polarization reversal of ferroelectric capacitor demonstrating negative capacitance-like behavior

Eisuke Tokumitsu*

School of Materials Science, Japan Advanced Institute of Science and Technology, 1-1 Asahisai, Nomi, Ishikawa 923-1292, Japan

*E-mail: e-toku@jaist.ac.jp

Received July 17, 2019; revised September 26, 2019; accepted October 11, 2019; published online December 4, 2019

Polarization reversal of a ferroelectric capacitor with a load resistance has been calculated by the Kolmogorov–Avrami–Ishibashi (KAI) model. Polarization change, current response and voltage across the ferroelectric capacitor were calculated and then the total charge density was plotted as a function of voltage across the ferroelectric capacitor to reconstruct polarization-electric field relation. Negative capacitance-like behavior was observed due to the voltage drop across the load resistance caused by the switching current of ferroelectric polarization reversal. In addition, circuit and switching parameter dependences on the negative capacitance-like behavior are discussed. It is shown that a dimensionality factor in the KAI model formulation affects the negative capacitance-like behavior. The presented calculation results indicate that the switching current during the polarization reversal is important to observe the negative capacitance-like behavior in the pulse response of the RC circuit with a ferroelectric capacitor, which is essentially different from the originally proposed concept of negative capacitance.

1. Introduction

A ferroelectric material is defined as a material that has spontaneous polarization and it can be reversed by an external electric field. Therefore, the ferroelectric material itself contains non-volatile memory function. Research on ferroelectric non-volatile random access memory (FeRAM) has been actively conducted since the 1980s and FeRAM is commercially available at present.[1,2] Commercially available FeRAM is a "capacitor type" having a cell structure of a ferroelectric capacitor and a select transistor as in a conventional DRAM memory cell. The other type of FeRAM is a "transistor type", in which ferroelectric-gate transistors are used as memory elements as in flash memory. The idea of ferroelectric-gate structure was proposed as early as 1957[3] and the first experimental results were reported in 1963.[4] A lot of work has been carried out on the ferroelectric-gate transistor, mainly based on Si technology using ferroelectric materials such as $Pb(Zr,Ti)O_3$ (PZT), $SrBi_2Ta_2O_9$ (SBT) and $(Bi,La)_4Ti_3O_{12}$ (BLT).[5–14] The transistor-type FeRAM has the potential for future non-volatile memory applications because of the nondestructive readout and its scalability.[15] In particular, because of the recent discovery of HfO_2-based ferroelectrics,[16–18] the ferroelectric-gate transistor has been highlighted again. Since HfO_2 has much larger coercive field than the conventional ferroelectric materials, an appropriate memory window can be obtained when it is used as a gate insulator in Si metal-oxide-semiconductor field-effect transistors (MOSFETs), even if the thickness is as thin as 10 nm. In addition, HfO_2 is compatible with the Si MOSFET fabrication process. These features make HfO_2 promising for ferroelectric-gate transistor applications.

In addition to the non-volatile memory function, the ferroelectric exhibits a "unique" physical property where the amount of charge density which can be induced is much larger than that of a conventional paraelectric material. For instance, the maximum available charge density of SiO_2 is limited to 3.5 $\mu C\,cm^{-2}$, assuming a breakdown voltage of 10 $MV\,cm^{-1}$, whereas the polarization value of ferroelectric material is as high as 10–50 $\mu C\,cm^{-2}$ even at an applied electric field of less than 1 $MV\,cm^{-1}$. This is about ten times larger than the maximum induced charge amount of SiO_2. The authors focused on this feature and realized a thin-film transistor using ITO of conductive oxide as a channel[19,20]

More recently, there is another trend in ferroelectric-gate transistor; the use of ferroelectric-gate structure for steep-slope transistor. The subthreshold voltage swing (SS) of MOSFET is given by the following equation,

$$SS = \frac{dV_{GS}}{d\,\log I_D} \approx \ln 10 \cdot \frac{kT}{q}\left(1 + \frac{C_D}{C_{OX}}\right), \qquad (1)$$

where k is the Boltzmann constant, q the elemental charge, C_D the depletion capacitance and C_{OX} the oxide capacitance, respectively. When the capacitance of the gate insulator is large and the second term of the parenthesis is negligible, the SS will be 60 mV $decade^{-1}$ at 300 K. This is the theoretical limit for conventional MOSFET and now one of the obstacles for further low-voltage operation for Si MOSFETs. Hence, there is a demand to realize a transistor with a low SS value less than 60 mV $decade^{-1}$ at 300 K and such a transistor is called a steep-slope transistor. As can be understood from Eq. (1), if the Cox were negative, the SS could be less than 60 mV $decade^{-1}$ at 300 K. Salahuddin and Datta[21] claimed that since a theoretical approach based on Landau theory of phase transitions to explain the hysteresis characteristics of ferroelectrics indicates an S-shaped relationship between polarization and electric field, if it is possible to use a region showing negative capacitance ($dQ/dE < 0$), an SS can be lower than the theoretical limit. However, one should note that such a negative capacitance region is usually unstable and not observed. It is claimed that a series connection of paraelectric capacitor is required to stabilize the negative capacitance effect.[22] One of the recent reports[23] clearly shows a capacitance of ferroelectric/paraelectric stacked capacitor is lower than that of the ferroelectric or paraelectric capacitor itself, which does not support the negative capacitance concept. So far, many papers have reported on both experimental and theoretical considerations[24–29] of the negative capacitance concept, and low SS values less than 60 mV $decade^{-1}$ have been reported.[30,31] In spite of many publications, the mechanism of negative capacitance is still under discussion.[29,32]

When the idea of negative capacitance effect was proposed, since it employs the S-shaped theoretical curve, it was a quasi-static effect. On the other hand, recent reports analyze dynamic behavior including the polarization reversal of ferroelectric. One of the appropriate approaches is to measure the current response when short voltage pulses are applied to the ferroelectric capacitor. Khan et al. measured the pulse response of the RC circuit with a ferroelectric capacitor and observed a sharp decrease in the voltage of the ferroelectric capacitor.[25)] They concluded that the observed decrease in voltage of the ferroelectric capacitor was direct evidence of negative capacitance. Kim et al. also observed a decrease in voltage across the ferroelectric capacitor in the pulse response and discussed the mechanism of the polarization reversal by fitting the experimentally observed current response with simulation.[28)] In this paper, we present a simpler view of pulse response of the ferroelectric capacitor, which demonstrates negative capacitance-like behavior, by analyzing the switching current of the ferroelectric polarization reversal. It is suggested that the decrease in the voltage of the ferroelectric capacitor can be understood by simply considering the voltage drop across the load resistor, which was connected in series in the RC circuit.

2. Calculation procedure

Figure 1 shows a circuit used for calculation, which consists of a series connection of a load resistor and a ferroelectric capacitor that has both paraelectric and ferroelectric components. This is the same circuit as that experimentally used to measure the pulse response in the literature.[25,27,28)] When we apply the voltage pulse sequence to the circuit, the current response, as schematically shown in Fig. 2(a), will be obtained. When a negative voltage pulse is applied at first to reset the polarization, the polarization moves to point C in Fig. 2(b) and goes to point B after the voltage is returned to zero. Here, the polarization value is –Pr (Pr:remanent polarization). Then, subsequently, when a positive voltage pulse is applied, the polarization moves to point D and goes to point A after the voltage pulse. Since the polarization of point A is +Pr, the total charge difference in the movement from B to A is 2Pr, as shown in Fig. 2(b), which appears as switching current. By integrating the switching current over time, 2Pr can be deduced. It should be noted that the total current response consists of the switching current and non-switching current for the first positive pulse. For a second positive voltage pulse, the operation point moves from A to D and returns to A again. In this case, only non-switching current flows and no switching current is observed. In this work, the current response was calculated for the first positive pulse, which contains the polarization reversal of the ferroelectric material. Then, the voltage applied to the ferroelectric capacitor is estimated as a function of time, considering the voltage drop of the load resistor. Finally, total charge density, Q, was plotted as a function of voltage across the ferroelectric capacitor, V_F, to reconstruct polarization-electric field (P-E) characteristics.

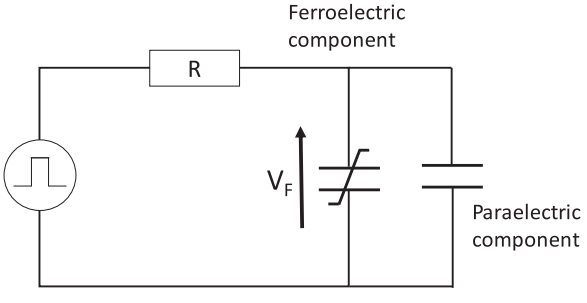

Fig. 1. RC circuit used for calculation.

Polarization reversal of the ferroelectric capacitor has been calculated using the Kolmogorov–Avrami–Ishibashi (KAI) model.[33)] In this model, the polarization reversal of the multigrain structure can be considered, whereas the so-called Landau theory, which explains the P-E hysteresis by an S-shaped curve, assumes homogenous polarization reversal of the film. In the KAI model, polarization reversal proceeds in the following manner. Suppose the positive voltage is applied for polarization reversal to the film which was initially polarized –Pr completely. (i) First, nuclei of +P are formed at the electrode/film interface. (ii) Second, nuclei grow and penetrate the film and +Pr domains appear. (iii) Third, the domain walls move laterally and the area of +Pr domains increase. (iv) Finally, +Pr domains collide with each other and the whole area of the film becomes +Pr, which means that the polarization reversal is completed. The switching time of the polarization reversal is determined by the lateral growth of the +Pr domains. According to this model, the intermediate state of the P-E hysteresis curve can be understood by the area ratio of +Pr domains to –Pr domains. This picture is different to that predicted by the Landau theory.

The polarization change as a function of time can be expressed as,

$$P = Pr\left\{1 - 2\exp\left[-\left(\frac{t}{t_s}\right)^n\right]\right\}, \tag{2}$$

where Pr, t_s and n mean remanent polarization, switching time and the dimensionality (or shape) factor, respectively. By differentiating Eq. (2) by time, the switching current during the polarization reversal can be calculated. Note that the pulse response of the ferroelectric capacitor has basically two components, switching current and non-switching current, as shown in Fig. 2, because the capacitor has ferroelectric and paraelectric components. The total current response is obtained by the sum of these two current components.

The analyzed circuit consists of a series connection of a load resistor and a ferroelectric capacitor that has both paraelectric and ferroelectric components, as shown in Fig. 1. The assumed remanent polarization, relative dielectric constant and thickness are 20 μC cm^{-2}, 20 and 10 nm, respectively, based on HfO_2-based ferroelectric materials. We assume a 3 V, 1 or 1.5 μs pulse is applied to the series connection of a load resistor (0.5 or 1 kΩ) and a ferroelectric capacitor with an area of 50 × 50 μm^2. Switching time was set at either of 300 or 600 ns and assumed as a constant for simplicity. It was reported that good agreement was obtained between the experimentally observed current response of ferroelectric PZT films and the calculated response by the KAI model for a constant switching time.[34,35)]

In this work, pulse response was calculated by the KAI model and Q–V_F relation (P-E hysteresis loop) was constructed as follows:

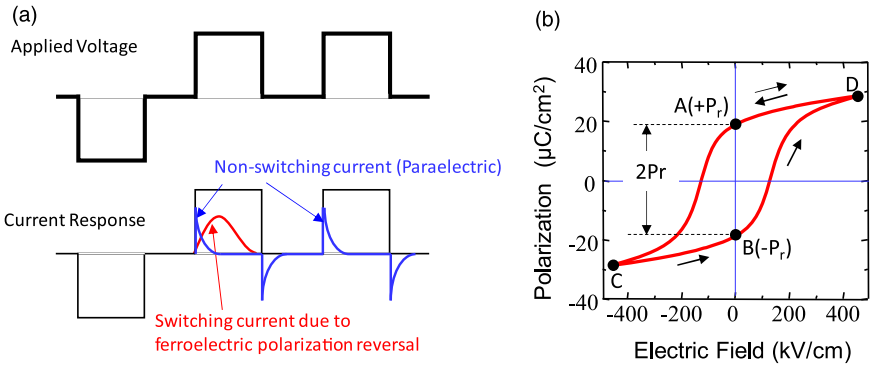

Fig. 2. (Color online) Schematic illustration of (a) applied pulse sequence and current response and (b) corresponding operation points in the P-E loop.

(1) calculate polarization as a function of time using Eq. (2),
(2) calculate switching current by differentiating Eq. (2) over time
(3) calculate total current (switching current + non-switching current),
(4) calculate voltage applied to the ferroelectric capacitor, V_F by an equation $V_F = V - R \cdot I$, where V is voltage of power supply, R is load resistance and I is current flow through R.
(5) Construct Q–V_F curve, by plotting the total charge density (polarization + non-switching charge) as a function of the voltage of the ferroelectric capacitor, V_F. Charge density in the negative V_F region is duplicated symmetrically.

Note that the voltage across the ferroelectric capacitor is determined by $V_F = V - R \cdot I$, which is key to causing the decrease in V_F and negative capacitance-like behavior.

3. Results and discussion

3.1. Pulse response and construction of Q–V_F relation

Here, we show details of calculation of the pulse response and construction of the Q–V_F relation (P-E loop). The parameters used for calculation are $t_s = 300$ ns, $R = 1$ kΩ and $n = 2.0$. Figure 3(a) shows the calculated polarization as a function of time using Eq. (2). It is shown that the polarization was varied from -Pr to +Pr with time. The shape of the curve is dependent on the dimensionality factor n, as shown later. Then, by differentiating the polarization over time, we obtain the "switching" current, as shown in Fig. 3(b), which has a peak around 200 ns. Then, the total current response was obtained by the addition of the "switching" current and "non-switching" current. The "non-switching" current is expressed by $(V/R)\exp(-t/\tau)$, where τ is a time constant determined by the RC product (R is the load resistance and C is the paraelectric component capacitance of the ferroelectric capacitor). Using the combination of the parameters used in the calculation, the obtained current response is shown in Fig. 3(c). It is shown that large current flows instantaneously when the voltage pulse is applied ($t = 0$) and decreases with time because of the paraelectric component (non-switching current). Then, the current increases with time because the switching current starts to flow and has a peak around 200 ns and decreases again. This calculation result shows typical current response of the ferroelectric capacitor. Next, the voltage applied to the ferroelectric capacitor can be obtained by the $V_F = V$–RI relation. Fig. 3(d) shows the voltage applied to the capacitor as a function of time (solid line). For comparison, the voltage response when only the paraelectric component is considered, is also shown by the dotted line in the figure. It can be seen that the voltage increases initially, but soon decreases with time. This behavior directly corresponds to the current response where the switching current starts to flow. A similar response was reported experimentally.[25,27,36] Since the voltage across the ferroelectric capacitor is given by $V_F = V$–RI relation, V_F variation with time is a "mirror image" of the current response. Then, the voltage increased again and finally reached the voltage equal to the supply voltage ($V = 3$ V). When we plot the total charge density including the switching charge and non-switching charge as a function of time, the result is shown in Fig. 3(e). The total charge density was calculated by adding the non-switching charge and switching charge, which increases monotonically as a function of time. On the other hand, the voltage applied to the ferroelectric capacitor decreases for the region of approximately 50–200 ns. It is possible that the ferroelectric capacitor has a negative capacitance in this range. However, it should be noted that the voltage decrease of the ferroelectric capacitor in this range is caused by the voltage drop of the load resistor due to the switching current flow. This does not mean the negative capacitance of the ferroelectric material itself. If we plot the total charge density, Q, shown in Fig. 3(e), as a function of the voltage across the ferroelectric capacitor, V_F, shown in Fig. 3(d), we can obtain the Q–V_F relation, as shown in Fig. 3(f), which corresponds to the P-E hysteresis loop of the ferroelectric material. As can be clearly seen in this figure, negative capacitance-like behavior was observed in the Q–V_F relation. We would like to point out again that this negative capacitance-like behavior is caused by the circuit pulse response, not by the negative capacitance of the ferroelectric material itself, although the constructed Q–V_F relation looks as though the S-shaped curves appeared. A key phenomenon for such negative capacitance-like behavior is due to the fact that switching current flows by the polarization reversal. This switching current generates the voltage drop across the load resistor, which causes the voltage decrease across the ferroelectric capacitor.

3.2. Effect of load resistance

Since the calculated negative capacitance-like behavior is due to the voltage drop of the resistance in the RC series circuit, we calculated the pulse response with different load

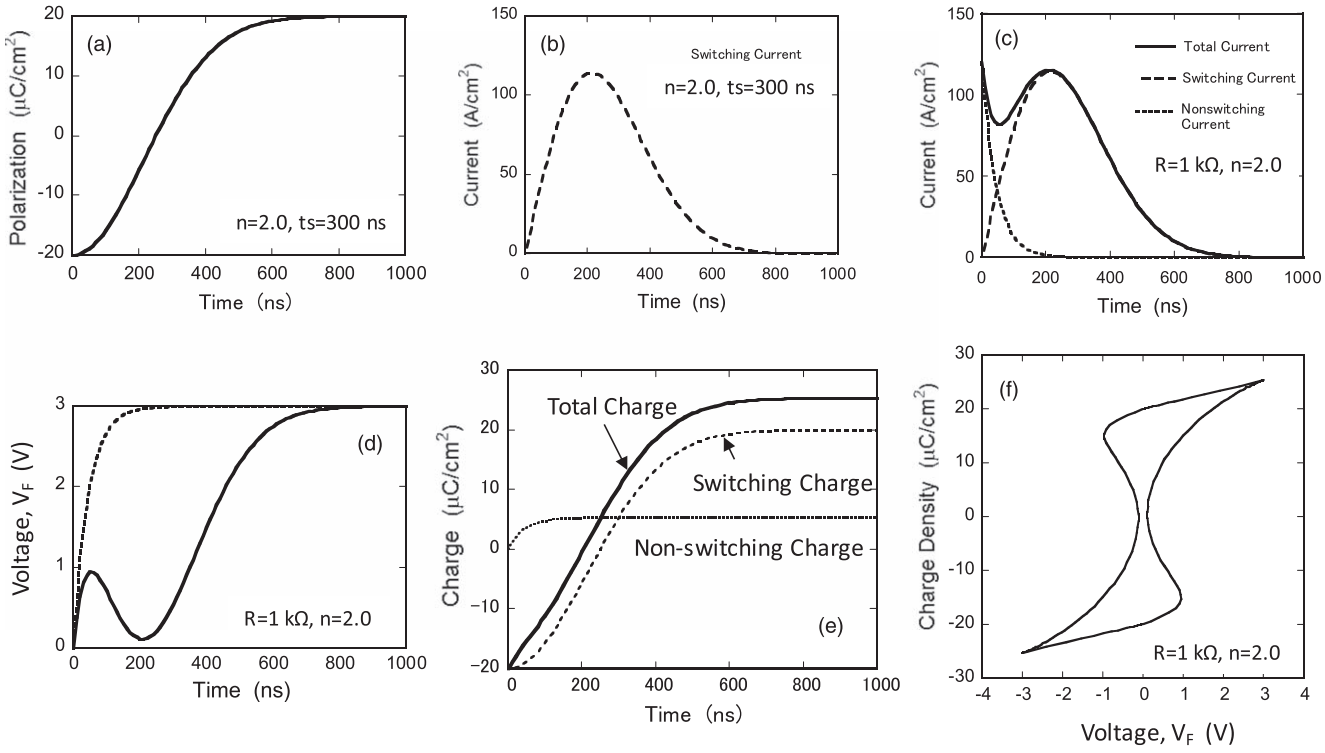

Fig. 3. Calculated (a) switching charge density, (b) switching current density, (c) total current density, (d) voltage across the ferroelectric capacitor, V_F, (e) total charge density and (f) constructed charge density–voltage of the ferroelectric capacitor (Q–V_F) relation, which corresponds to the P-E loop of ferroelectric material. Parameters used for calculation are $t_s = 300$ ns, $R = 1$ kΩ and $n = 2.0$.

resistance. Figure 4(a) shows current response when the load resistance is 500 Ω. When the load resistance was reduced, the time constant of paraelectric component RC was reduced and the initial current value increased. As a result, the current response shape is different to that for $R = 1$ kΩ. In addition, the voltage drop across the resistor is reduced and the voltage change of the ferroelectric capacitor over time was distorted, as shown in Fig. 4(b). As shown in Fig. 4(b), the voltage at the valley point is larger and the valley is not steep in this case because of the small voltage drop of the load resistance ($R = 500$ Ω). Therefore, a constructed Q–V_F relation looks to have less pronounced negative capacitance-like characteristics, as shown in Fig. 4(c). A similar effect is also seen when the capacitance area was reduced. When the area of the ferroelectric capacitor was reduced, the RC time constant decreases since the capacitance was reduced. In this case, the switching current was also reduced because the ferroelectric capacitor area was reduced. Consequently, the voltage drop of the load resistance was reduced and a similar Q–V_F relation, as shown in Fig. 4(c), was obtained.

3.3. Effect of switching time

As discussed in the previous section, the combination of the switching and non-switching current components is important to observe the negative capacitance-like behavior. We next varied the switching time. Figure 5(a) shows the current response when the switching time is increased from 300 to 600 ns. The other parameters are the same ($R = 1$ kΩ, area $= 50 \times 50\ \mu m^2$ and $n = 2.0$). Since the switching time was increased to 600 ns, the peak of the switching current moved to a longer time region and the peak current was also decreased. According to the smaller peak of the switching current, the valley of the voltage change of the ferroelectric

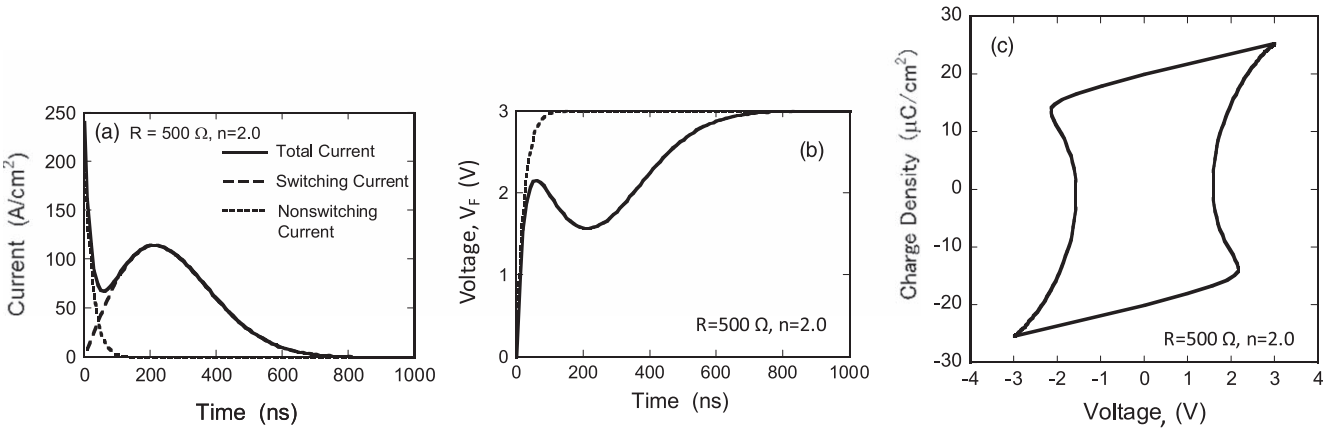

Fig. 4. Calculated (a) total current density along with switching and non-switching current, (b) voltage across the ferroelectric capacitor, V_F, and (c) constructed Q–V_F relation for $t_s = 300$ ns, $R = 500$ Ω and $n = 2.0$.

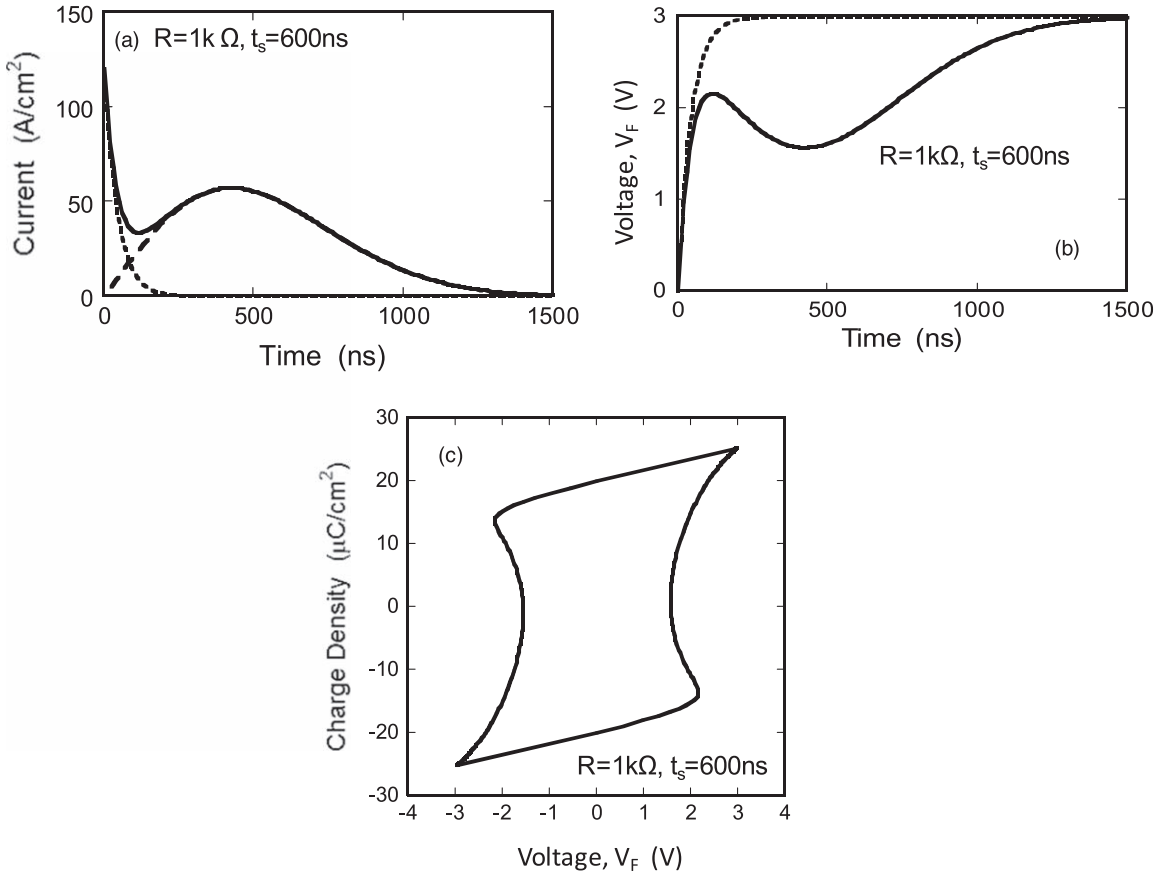

Fig. 5. Calculated (a) total current density along with switching and non-switching current, (b) voltage across the ferroelectric capacitor, V_F, and (c) constructed Q–V_F relation for $t_s = 600$ ns, $R = 1$ kΩ and $n = 2.0$.

capacitor is not steep, as shown in Fig. 5(b). Consequently, a constructed Q–V_F relation, shown in Fig. 5(c), is similar to that shown in Fig. 4(c). This result also shows the importance of the combination of the switching and non-switching current component to observe the negative capacitance-like behavior.

3.4. Dimensionality factor dependence

It is interesting to examine how the dimensionality (or shape) factor, n, of Eq. (2) during the ferroelectric polarization reversal affects the current response and negative capacitance-like behavior. Figure 6(a) shows polarization change as a function of time for $n = 1.5$, 2.0 and 3.0, respectively. It is shown that when the dimensionality factor is small, the polarization starts to increase from $t = 0$ and then, the polarization increases gradually. On the other hand, when $n = 3.0$, there is an incubation time in the beginning after which the polarization increases rapidly. According to these features, the switching current response is dependent on the dimensionality factor, as shown in Fig. 6(b). When $n = 1.5$, the switching current increases from $t = 0$, whereas the current starts to increase rapidly after the incubation time when $n = 3.0$. The peak of the switching current is located at late time regime for the large dimensionality factor. In addition, the peak value of the switching current is also large for large n.

Figures 7 and 8 show (a) current response, (b) voltage of the ferroelectric capacitor and (c) constructed Q–V_F relation, calculated for $n = 3.0$ and 1.5, respectively. When $n = 3.0$, the switching current and non-switching current were separated and the total current response has a clear peak, as shown in Fig. 7(a), because the switching current response is delayed. According to this, the voltage across the

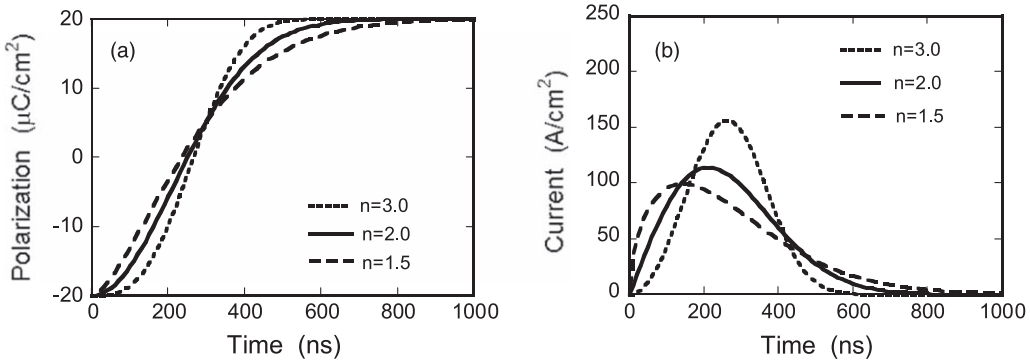

Fig. 6. (a) Charge density (polarization) change and (b) switching current response as a function of time for $n = 1.5$, 2.0 and 3.0.

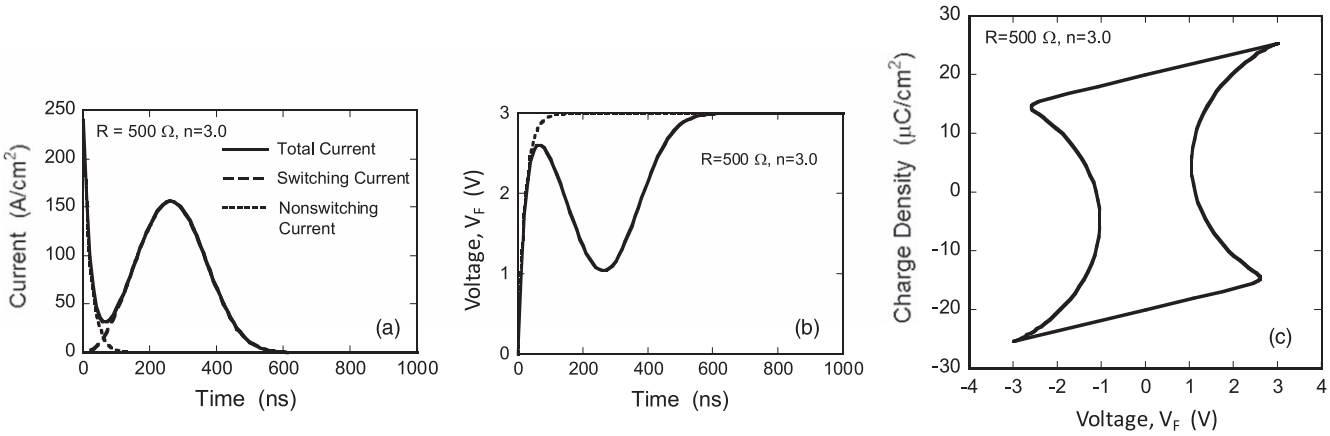

Fig. 7. Calculated (a) total current density along with switching and non-switching current, (b) voltage across the ferroelectric capacitor, V_F, and (c) constructed Q–V_F relation for $t_s = 300$ ns, $R = 500$ Ω and $n = 3.0$.

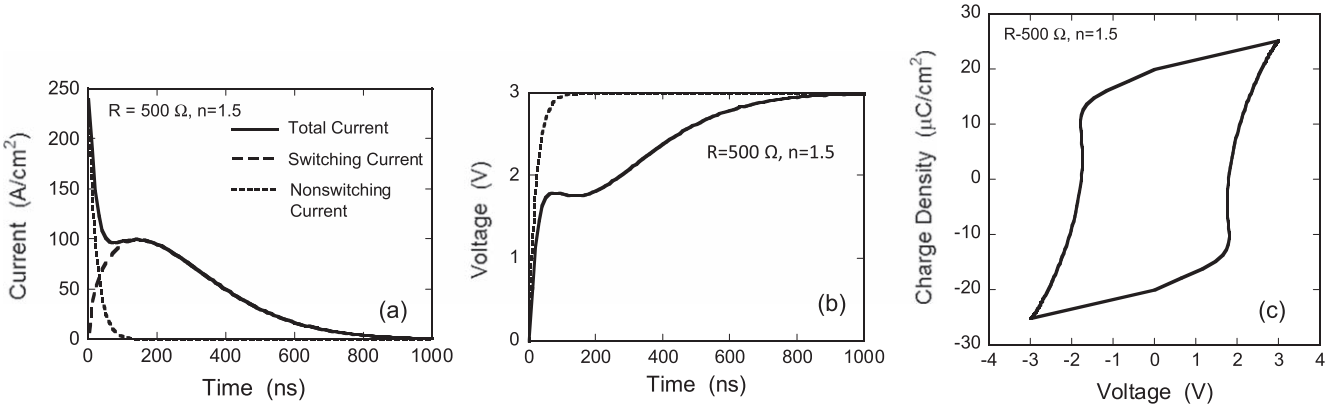

Fig. 8. Calculated (a) total current density along with switching and non-switching current, (b) voltage across the ferroelectric capacitor, V_F, and (c) constructed Q–V_F relation for $t_s = 300$ ns, $R = 500$ Ω and $n = 1.5$.

ferroelectric capacitor also has a clear valley and the pronounced negative capacitance-like behavior is observed in the Q–V_F relation, as shown in Fig. 7(c). On the other hand, when $n = 1.5$, since the peak of the switching current is located at a shorter time region, the switching current is partly merged with the non-switching current, as shown in Fig. 8(a). Under such a condition, there is almost no peak in the current response. Then, in the voltage V_F response, there is only a slight decrease, as can be seen in Fig. 8(b). Hence, only a slight negative capacitance effect is observed in the Q–V_F relation, as shown in Fig. 8(c). In summary, the negative capacitance-like behavior strongly depends on the dimensionality factor, n, of Eq. (2). This is because the switching current behavior has strong dependence on n. To observe the negative capacitance-like behavior clearly, large n value is preferable, because the current response shows large peak current at the late time region. Of course, other parameters such as RC time constant also affect the negative capacitance-like behavior.

It is interesting to consider what kinds of materials are suitable to observe negative capacitance-like behavior in the pulse response measurement of the RC circuit. To observe the effect, the switching current and non-switching current should be separated, which results in a clear decrease in the voltage response of the ferroelectric capacitor. To realize this situation, the RC time constant of the non-switching current should be small enough and the peak of the switching current should be located in relatively late time. To obtain a small RC time constant, a ferroelectric material with low dielectric constant of paraelectric component, such as HfO_2-based ferroelectrics, is preferable, compared to the conventional ferroelectric materials such as PZT. In fact, in our previous experimental observation of ferroelectric PZT capacitors, it was difficult to observe the separate current response because of the large RC time constant.[35] Of course, the RC time constant can be reduced by using small R or small area of the capacitor, but small R weakens the negative capacitance-like effect, as shown in Figs. 3 and 4. Hence, proper choice of R is also important. On the other hand, to obtain the delayed switching current, a ferroelectric material with a large n value is preferable, as shown in Figs. 7 and 8, provided that the polarization reversal process obeys the KAI model. In our old work,[35] it was shown that dimensionality factor, n, of the PZT films prepared by the sol–gel technique was around 1.3, whereas that of the PZT films prepared by vacuum evaporation was as large as 2.1. This means that ferroelectric domains of the sol–gel-derived PZT films grow one-dimensionally because 2D domain growth is suppressed probably due to the small grain size, whereas the planar growth of the ferroelectric domains is dominant in the PZT films prepared by vacuum evaporation. According to these considerations, it is suggested that ferroelectric materials which have small dielectric constant and good crystallinity with large grain size are suitable for the observation of negative capacitance-like

behavior in the transient pulse measurements of the RC circuit.

4. Conclusion

Pulse response of an RC circuit consisting of a load resistor and a ferroelectric capacitor with a paraelectric component was analyzed. To describe the polarization reversal as a function of time, the KAI model was used. The current response, charge density and the voltage applied to the ferroelectric capacitor were calculated. From these values, the Q–V_F relation, corresponding to P-E hysteresis was constructed. It was demonstrated that negative capacitance-like behavior can be observed in the Q–V_F relation by simply considering the voltage drop of the load resistor caused by the switching current of the ferroelectric capacitor. To observe the negative capacitance-like behavior clearly, the RC constant should be sufficiently short and large switching current is preferable. In addition, the load resistance should be properly chosen. It was also shown that the dimensionality factor affects the negative capacitance-like behavior. When a positive pulse is applied to the ferroelectric capacitor after the negative reset pulse was applied, switching current flows in the RC circuit due to polarization reversal. This work indicates that the switching current plays an important role in observing negative capacitance-like behavior whatever the polarization reversal mechanism is, and that the presented mechanism is essentially different to the originally proposed concept of negative capacitance.

Acknowledgments

This work is partially supported by the Mitani Foundation for Research and Development and the Izumi Science and Technology Foundation.

1) H. Ishiwara, M. Okuyama, and Y. Arimoto (ed.) *Ferroelectric Random Access Memories, Fundamentals and Applications* (Springer, Berlin, 2004).
2) M. Okuyama and Y. Ishibashi (ed.) *Ferroelectric Thin Films, Basic Properties and Device Physics for Memory Applications* (Springer, Berlin, 2005).
3) I. M. Loss, US Patent 2791760 (1957).
4) J. L. Moll and Y. Tarui, IEEE Trans. Electron Devices **ED-10**, 333 (1963).
5) Y. Higuma, Y. Matsui, M. Okuyama, T. Nakagawa, and Y. Hamakawa, Jpn. J. Appl. Phys. **17** [Suppl.17-1] 209 (1978).
6) E. Tokumitsu, G. Fujii, and H. Ishiwara, Appl. Phys. Lett. **75**, 575 (1999).
7) T. Hirai, Y. Fujisaki, K. Nagashima, H. Koike, and Y. Tarui, Jpn. J. Appl. Phys. **36**, 5908 (1997).
8) Y. Nakao, T. Nakamura, A. Kamisawa, and H. Takasu, Integr. Ferroelectr. **6**, 23 (1995).
9) Y. Fujimori, T. Nakamura, and A. Kamisawa, Jpn. J. Appl. Phys. **38**, 2285 (1999).
10) E. Tokumitsu, R. Nakamura, and H. Ishiwara, IEEE Electron Device Lett. **EDL-18**, 160 (1997).
11) E. Tokumitsu, G. Fujii, and H. Ishiwara, Jpn. J. Appl. Phys. **39**, 2125 (2000).
12) E. Tokumitsu, K. Okamoto, and H. Ishiwara, Jpn. J. Appl. Phys. **40**, 2917 (2001).
13) K. Aizawa, B.-E. Park, Y. Kawashima, K. Takahashi, and H. Ishiwara, Appl. Phys. Lett. **85**, 3199 (2004).
14) M. Takahash and S. Sakai, Jpn. J. Appl. Phys. **44**, L800 (2005).
15) X. Zhang, M. Takahashi, K. Takeuchi, and S. Sakai, Jpn. J. Appl. Phys. **51**, 04DD01 (2011).
16) T. S. Böscke, J. Müller, D. Bräuhaus, U. Schröder, and U. Böttger, Appl. Phys. Lett. **99**, 102903 (2011).
17) J. Müller, T. S. Böscke, D. Bräuhaus, U. Schröder, U. Böttger, J. Sundqvist, P. Kücher, T. Mikolajick, and L. Frey, Appl. Phys. Lett. **99**, 112901 (2011).
18) U. Schröder, E. Yurchuk, J. Müller, D. Martin, T. Schenk, P. Polakowski, C. Adelmann, M. I. Popovici, S. V. Kalinin, and T. Mikolajick, Jpn. J. Appl. Phys. **53**, 08LE02 (2014).
19) E. Tokumitsu, M. Senoo, and T. Miyasako, Microelectron. Eng. **80**, 305 (2005).
20) T. Miyasako, M. Senoo, and E. Tokumitsu, Appl. Phys. Lett. **86**, 162902 (2005).
21) S. Salahuddin and S. Datta, Nano Lett. **8**, 405 (2008).
22) D. J. R. Appleby, N. K. Ponon, K. S. K. Kwa, B. Zou, P. K. Petrov, T. Wang, N. M. Alford, and A. O'Neill, Nano Lett. **14**, 3864 (2014).
23) M. Si, X. Lyu, and P. D. Ye, ACS Appl. Electron. Mater. **1**, 745 (2019).
24) A. I. Khan, D. Bhowmik, P. Yu, S. J. Kim, X. Pan, R. Ramesh, and S. Salahuddin, Appl. Phys. Lett. **99**, 113501 (2011).
25) A. I. Khan, K. Chatterjee, B. Wang, S. Drapcho, L. You, C. Serrao, S. R. Bakaul, R. Ramesh, and S. Salahuddin, Nat. Mater. **14**, 182 (2015).
26) M. Hoffman, F. P. G. Fengler, M. Herzig, T. Mittmann, B. Max, U. Schröder, R. Negrea, P. Lucian, S. Slesazeck, and T. Mikolajick, Nature **565**, 464 (2019).
27) M. Hoffmann, A. I. Khan, C. Serrao, Z. Lu, S. Salahuddin, M. Pesic, S. Slesazeck, U. Schroeder, and T. Mikolajick, J. Appl. Phys. **123**, 184101 (2018).
28) Y. J. Kim, H. W. Park, S. D. Hyun, H. J. Kim, K. D. Kim, Y. H. Lee, T. Moon, Y. B. Lee, M. H. Park, and C. S. Hwang, Nano Lett. **17**, 7796 (2017).
29) M. A. Alam, M. Si, and P. D. Ye, Appl. Phys. Lett. **114**, 090401 (2019).
30) M. H. Lee et al., Tech. Digest Int. Electron Device Meeting (IEDM) 2015, pp. 616–9.
31) K. S. Li et al., Tech. Digest Int. Electron Device Meeting (IEDM) 2015, pp. 620–3.
32) K. Takada, T. Yoshimura, and N. Fujimura, AIP Adv. **9**, 025037 (2019).
33) Y. Ishibashi and Y. Takagi, J. Phys. Soc. Jpn. **31**, 506 (1971).
34) E. Tokumitsu, N. Tanisake, and H. Ishiwara, Jpn. J. Appl. Phys. **33**, 5201 (1994).
35) E. Tokumitsu, R. Nakamura, K. Itani, and H. Ishiwara, Jpn. J. Appl. Phys. **34**, 1061 (1995).
36) M. Kobayashi, N. Ueyama, K. Jang, and T. Hiramoto, Tech. Digest Int. Electron Device Meeting (IEDM) 2016, pp. 314–7.